

Tracing early structure formation with massive starburst galaxies and their implications for reionization

Kentaro Nagamine¹, Renyue Cen², Steven R. Furlanetto³,
 Lars Hernquist⁴, Christopher Night⁴, Jeremiah P. Ostriker²,
 Masami Ouchi⁵

¹*University of California, San Diego, Email: knagamine@ucsd.edu*

²*Princeton University Observatory, ³California Institute of Technology,*

⁴*Harvard University, ⁵Space Telescope Science Institute*

Abstract

Cosmological hydrodynamic simulations have significantly improved over the past several years, and we have already shown that the observed properties of Lyman-break galaxies (LBGs) at $z = 3$ can be explained well by the massive galaxies in the simulations. Here we extend our study to $z = 6$ and show that we obtain good agreement for the LBGs at the bright-end of the luminosity function (LF). Our simulations also suggest that the cosmic star formation rate density has a peak at $z = 5\text{--}6$, and that the current LBG surveys at $z = 6$ are missing a significant number of faint galaxies that are dimmer than the current magnitude limit. Together, our results suggest that the universe could be reionized at $z = 6$ by the Pop II stars in ordinary galaxies.

We also estimate the LF of Lyman- α emitters (LAEs) at $z = 6$ by relating the star formation rate in the simulation to the Ly α luminosity. We find that the simulated LAE LFs agree with the observed data provided that the *net* escape fraction of Ly α photon is $f_{Ly\alpha} \leq 0.1$. We investigate two possible scenarios for this effect: (1) all sources in the simulation are uniformly dimmer by a factor of 10 through attenuation, and (2) one out of ten LAEs randomly lights up at a given moment. We show that the correlation strength of the LAE spatial distribution can possibly distinguish the two scenarios.

Key words: cosmology, theory, galaxy formation, star formation

1 Introduction

One of the main goals of computational cosmology is to draw a complete, self-consistent picture of galaxy formation from first principles. Given the matter fluctuations in the initial conditions that are motivated by the inflationary theories, we can simulate the evolution of structure and the formation of galaxies using the laws of gravity and hydrodynamics under the cosmological model that is suggested by the observations such as the WMAP (Spergel et al. 2003) and Type I supernovae (e.g. Riess et al. 1998; Perlmutter et al. 1999).

Over the past several years, cosmological hydrodynamic simulations have improved significantly, and the simulations are now able to reproduce reasonable population of galaxies whose properties we can directly compare to the actual observations. In a series of past publications (Nagamine 2002; Nagamine et al. 2004ab, 2005a; Night et al. 2005), we have shown that our hydrodynamic simulations can account for the properties of LBGs at $z = 3 - 6$ very well if we associate them with massive starburst galaxies embedded in massive dark matter halos. Nagamine et al. (2005b) also discussed the near-IR properties of massive galaxies and Extremely Red Objects (EROs) in the simulations. In this conference proceedings, we summarize the study of LBGs at $z = 6$ as well as the Lyman- α emitters (LAEs) in cosmological hydrodynamic simulations.

2 Cosmological Hydrodynamic Simulations

We utilize two different types of cosmological hydrodynamic simulations based on a cold dark matter model: an Eulerian mesh code TIGER (Cen, Nagamine & Ostriker 2004) with Total Variation Diminishing (TVD; Ryu et al. 1993) shock capturing scheme, and a Smoothed Particle Hydrodynamics (SPH) code GADGET-2 (Springel 2005) which employs a novel entropy-conserving formulation (Springel & Hernquist 2002). Both simulations include standard physical treatments such as radiative cooling/heating, uniform UV background radiation, supernova feedback, and star formation. The SPH simulation also includes feedback by galactic wind and a multiphase ISM model for star formation (Springel & Hernquist 2003a,b). At each time step of the simulation, some fraction of gas is converted to star particles based on a Schmidt-type law in regions of very high density to model galaxy formation. Each star particle is tagged with physical quantities such as stellar mass, formation time, and metallicity, which enable us to apply a population synthesis technique on each star particle and obtain luminosity output. Collections of star particles are identified with a grouping algorithm and identified as galaxies. Table 1 lists important parameters of the simulations, and we refer the readers to Nagamine et al. (2005a,b) for more details on particular simulation runs that we utilize

Run	Boxsize	$N_{\text{mesh/ptcl}}$	m_{DM}	m_{gas}	ϵ
SPH Q5	10.	324^3	2.1×10^6	3.3×10^5	1.2
SPH Q6	10.	486^3	6.3×10^5	9.7×10^4	0.8
SPH D5	33.75	324^3	8.2×10^7	1.3×10^7	4.2
SPH G6	100.	486^3	6.3×10^8	9.7×10^7	5.3
TVD N864L22	22.	864^3	8.9×10^6	2.2×10^5	25.5
TVD N1024L85	85.	1024^3	1.6×10^8	3.6×10^6	83.0

Table 1

SPH and TVD simulations employed in this study. The box size is in units of $h^{-1}\text{Mpc}$. For the SPH, the (initial) number of gas particles N_{P} is equal to the number of dark matter particles, so the total particle count is twice N_{ptcl} . m_{DM} and m_{gas} are the masses of dark matter and gas particles (mean baryonic mass per cell for TVD) in units of $h^{-1}M_{\odot}$, respectively. ϵ is the comoving gravitational softening length for the SPH (cell size for TVD) in units of $h^{-1}\text{kpc}$.

for our study. All simulations assume a standard flat Λ cosmology.

3 Galaxy LF at $z = 6$ & Cosmic Star Formation History

The luminosity function (LF) of simulated LBGs at $z = 6$ is shown in the left panel of Fig. 1. It shows that the simulated LF agrees well with the observed one by Bouwens et al. (2004) at the bright-end. It is encouraging that we obtain good agreement with observations for the LFs at $z = 3 - 6$ throughout, as well as with the rest-frame UV colors (Night et al. 2005). This suggests that the simulated LBGs have realistic star formation rates and histories compared to those of the actual LBGs. A notable feature of simulated LFs is that the faint-end slope is quite steep with $\alpha \simeq -2.0$ in the rest-frame magnitude range $-19 < M_{1350} < -16$. This magnitude range is even beyond the current magnitude limit of rest-frame $M_{1350} \simeq -19$.

In the right panel of Fig. 1, we show the cosmic star formation history as a function of redshift. Both hydro simulations (Nagamine et al. 2001, 2004b) and the model by Hernquist & Springel (2003) suggest that the peak of the SFR density is at $z \geq 5$, which is quite different from the predictions of some of the semi-analytic models (e.g. Kauffmann et al. 1999; Cole et al. 2000; Somerville et al. 2001; Menci et al. 2002). Together with the steep faint-end slope of the LF, our results suggest that there would be enough ionizing photons to reionize the Universe at $z = 6$ with the Pop II stars in standard galaxies (Nagamine et al. 2005, in preparation).

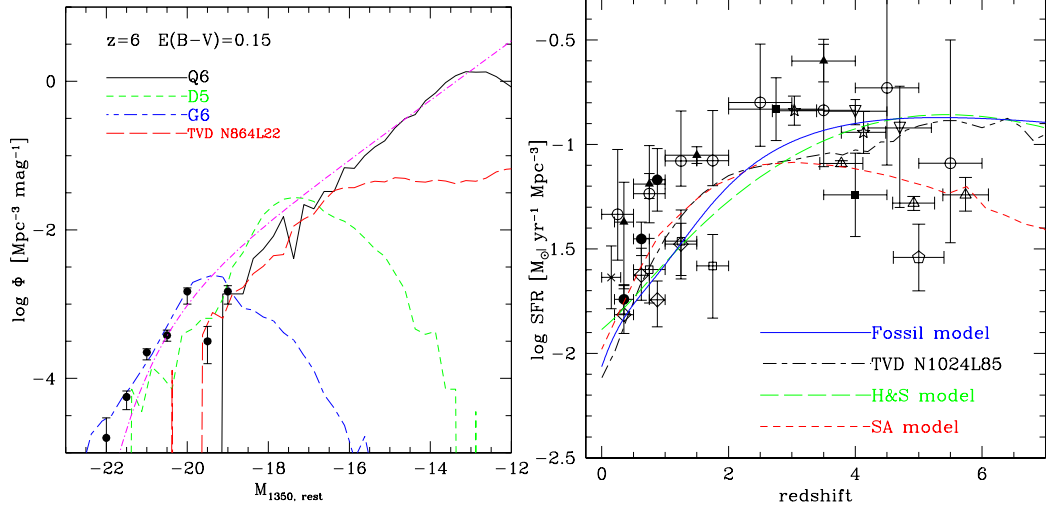


Fig. 1. *Left*: Luminosity function of galaxies at $z = 6$ in simulations. Uniform extinction of $E(B-V) = 0.15$ is assumed. Data points are from Bouwens et al. (2004). *Right*: Cosmic star formation history in hydro simulations and other models. Note that all models except the semianalytic model (SA model) have a peak of SFR density at $z \gtrsim 5$. H&S model is the one by Hernquist & Springel (2003) based on the results of SPH simulations. For the details on the extinction corrected data points, see Nagamine et al. (2004b). The ‘Fossil’ model is from Nagamine et al. (2005, in preparation).

4 Large-scale scale structure at $z = 6$ and Lyman- α Emitters

Figure 2 shows the projected dark matter density field at $z = 6$ (left) and 3 (right). The left panel shows that the large-scale structure is already roughly in place by $z = 6$ with large voids. Each panel has a size of comoving 143 Mpc on a side, corresponding to 1 degree at $z = 6$. The filaments become tighter and high density peaks become more prominent by $z = 3$. In our simulations, LBGs and LAEs are centered on high density peaks that appear bright in this figure. The figure shows that a large survey area (~ 1 degree) is needed in order to obtain a representative sample of LBGs or LAEs at $z = 6$. If a $(10 \text{ arcmin})^2$ field-of-view of a survey was (unluckily) placed on a void as shown in this picture, the number density of the source would be significantly underestimated relative to the cosmic mean due to a strong cosmic variance effect.

5 Luminosity function of LAEs at $z = 6$

We estimate the Ly α luminosity of each galaxy in the simulation from the instantaneous star formation rate using the relation $L_{\text{Ly}\alpha} = 10^{42} \text{ erg s}^{-1}$ per

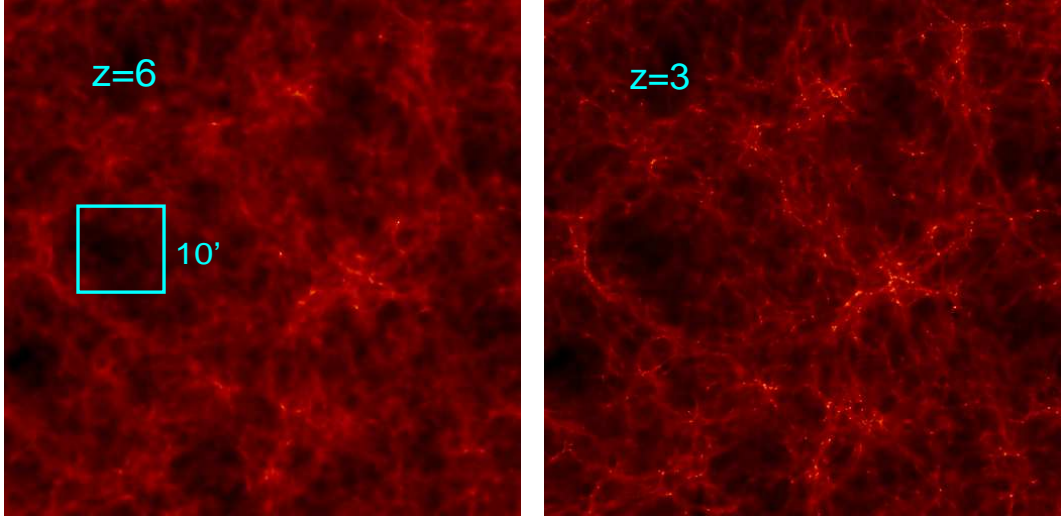


Fig. 2. Projected dark matter density field at $z = 6$ (left) and 3 (right) from the SPH G6 run. Each panel has a size of comoving 143 Mpc on a side, corresponding to 1 degree at $z = 6$. The small box in the left panel shows an example survey area of $(10 \text{ arcmin})^2$.

$1 M_\odot \text{ yr}^{-1}$ (e.g. Leitherer et al. 1999). This conversion factor could be higher if the IMF is top heavy. In the left panel of Figure 3, we show the cumulative luminosity function of LAEs at $z = 6$ estimated from the simulations as we described above. We find that the simulations overpredict the LF by a factor of ≈ 10 compared to the observational estimate by Ouchi et al. (2005b, in preparation) for the $z \sim 6$ LAE sample presented in Ouchi et al. (2005a). Since their field-of-view was ~ 1.5 degrees, the sample is large enough that it shouldn't be severely affected by the cosmic variance, and their result also agrees with that of Malhotra & Rhoads (2004) within the error bars. Furlanetto et al. (2005) have also found the same overestimate of LAE LF in simulations at lower redshifts.

There are at least two possible ways to reconcile the overprediction of the simulated LF relative to the observed one: (1) all the LAEs are attenuated by a factor of ~ 10 (hereafter ‘uniform dimming’ scenario), or (2) one out of ten LAEs randomly ‘turns on’ at a given time (hereafter ‘random sampling’ scenario). In the latter case, the reason for the randomness would be primarily due to the random geometry of the gas clouds around star-forming regions which block the Ly α photons traveling towards us, and not due to the fluctuation of star formation activity. The fluctuating SFR is already reflected in the distribution of the Ly α luminosity, and the simulation box is large enough to smooth out such fluctuations when averaged over the entire simulation volume. For these reasons, here we take the 1:10 ratio at face value as a random sampling of the sources and see what we can learn from this simple exercise. In the real Universe, a combination of the above two effects may be at play.

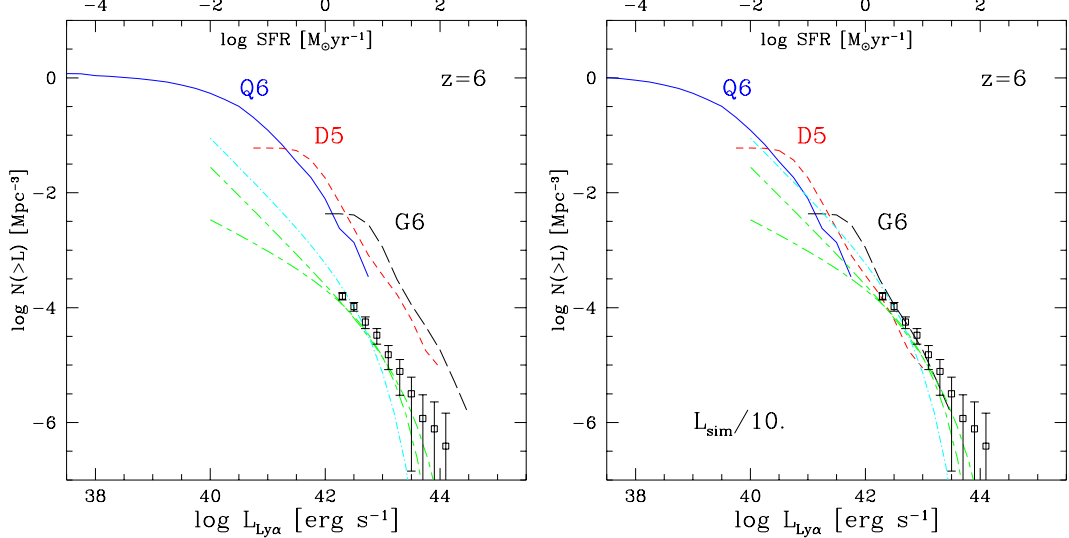


Fig. 3. Cumulative luminosity function of LAEs from 3 different SPH simulations. Left panel is directly estimated from the simulation using the method described in the text, and the right panel is the ‘uniform dimming’ scenario where all sources are dimmed by a factor of 10. The larger box-size simulation covers the brighter end of the LF due to more numerous massive halos.

The right panel of Fig. 3 shows the ‘uniform dimming’ scenario where all LAEs are uniformly dimmed by a factor of 10. This uniform dimming can be regarded as a *net* result of 3 different physical processes: First is the fact that a fraction f_{esc} of all ionizing photons escape from the galaxy and do not contribute to the creation of Ly α photons. Second is the dust attenuation by a factor of $e^{-\tau_{\text{dust}}}$. Third is that only a fraction f_{IGM} of Ly α photons penetrates the IGM and reaches us (e.g. Barton et al. 2004), although this effect is only significant before reionization ($z \gtrsim 6$). This can be summarized as follows: $F_{\text{Ly}\alpha, \text{obs}} = f_{\text{Ly}\alpha} F_{\text{Ly}\alpha, \text{em}} = e^{-\tau_{\text{dust}}} (1 - f_{\text{esc}}) f_{\text{IGM}} F_{\text{Ly}\alpha, \text{em}}$, where $f_{\text{Ly}\alpha}$ characterizes the *net* escape fraction of Ly α photons from LAEs. Our simulations suggest $f_{\text{Ly}\alpha} \sim 0.1$ for a conversion factor of $L_{\text{Ly}\alpha} = 10^{42} \text{ erg s}^{-1}$ per $1 M_{\odot} \text{ yr}^{-1}$. If the IMF is top heavy and the true value of the conversion factor is larger than the above, then the value of $f_{\text{Ly}\alpha}$ will become proportionally smaller.

6 Correlation function of LAEs

There is a possibility of distinguishing the two scenarios discussed in the previous section by looking at the correlation strength of the spatial distribution of LAEs. In the ‘uniform dimming’ scenario, the sources basically correspond to the brightest galaxies in the most massive halos, therefore they are as strongly clustered as the bright LBGs. In the ‘random sampling’ scenario, there are two effects that would weaken the clustering strength compared to the ‘uniform

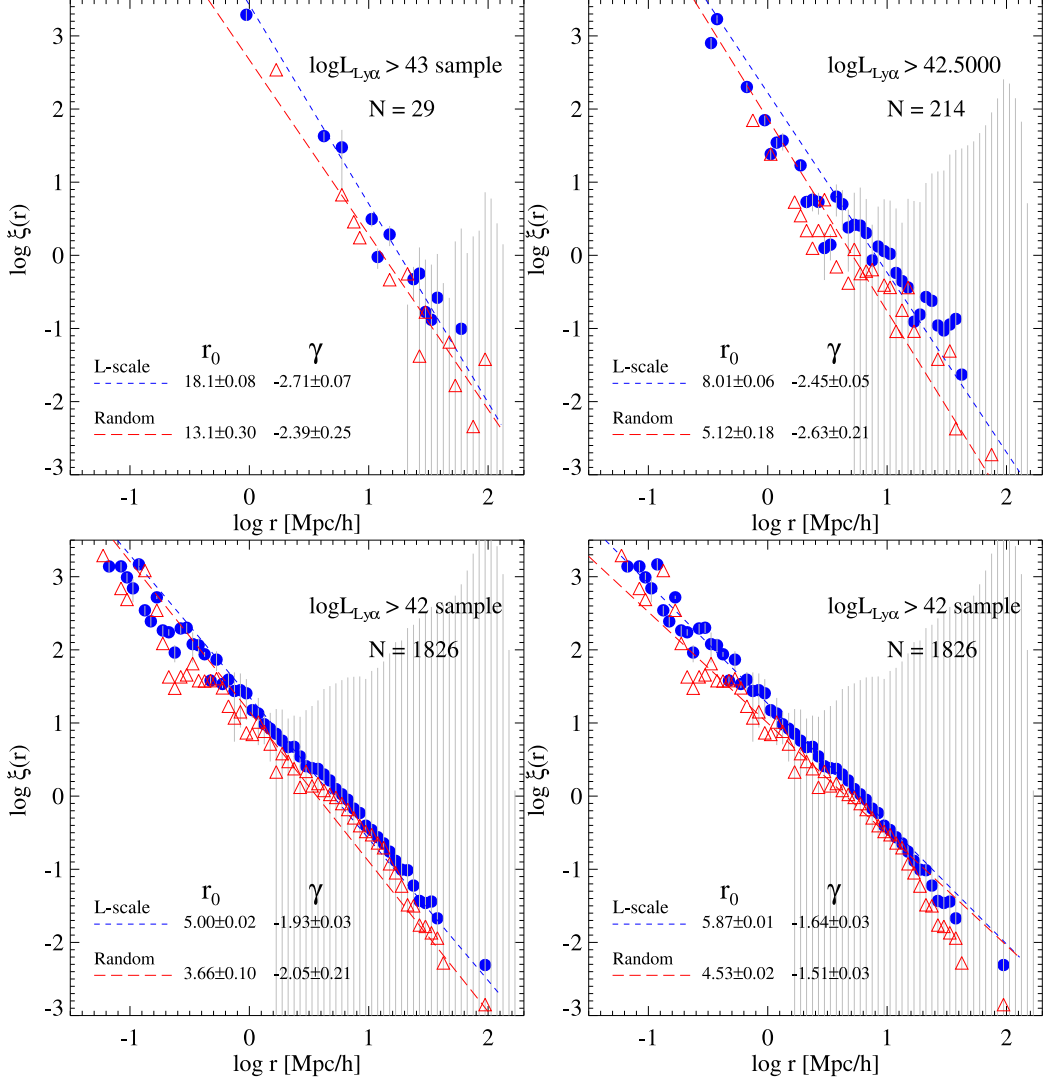


Fig. 4. Correlation function of simulated LAEs in SPH G6 run at $z = 6$ with different luminosity cuts. In all cases, the ‘uniform dimming’ case (solid circles and *short-dashed* line) has a longer correlation length r_0 than the ‘random sampling’ case (open triangles and *long-dashed* line). The bottom right panel uses the same sample as the bottom left panel, but the power-law fitting was performed to the data points limited to the range $-0.5 < \log r < 1.0$. The gray error bars are the standard deviations of the distribution for each bin based on the calculation of $\xi(r)$ for $2 \times 2 \times 2 = 8$ smaller subdivided simulation boxes. Therefore they include the effect of cosmic variance on scales of comoving $50 h^{-1}\text{Mpc}$, but not for larger scales.

dimming’ scenario: 1) the number of more massive halos that dominate the correlation signal is smaller in the randomly selected sample than the parent sample, because the number of lower luminosity LAEs that are hosted by lower mass halos is larger, and 2) Poisson noise is introduced by the random sampling.

This is demonstrated in Figure 4, where the spatial correlation function was computed in the two different scenarios for samples with different Ly α luminosity limit. In all cases, the ‘uniform dimming’ scenario (solid circles and the *short-dashed* line for the power-law fit) has a longer correlation length r_0 than the ‘random sampling’ case (open triangles and the *long-dashed* line). There does not seem to be a clear trend for the slope of the correlation function. Our predictions for the correlation lengths can be directly compared with observational data, and the above two scenarios can be tested in the near future.

7 Conclusions & Discussions

The main conclusions of my talk are the following:

- (1) Luminosity functions of simulated galaxies in cosmological hydro simulations agree well with those of the observed LBGs at $z = 3 - 6$ at the bright-end (Night et al. 2005). At $z = 6$, they have a steep faint-end slope of $\alpha \sim -2.0$ in the rest-frame magnitude range $-19 < M_{1350} < -16$. This magnitude range is even beyond the current magnitude limit of rest-frame $M_{1350} \simeq -19$.
- (2) Cosmological hydro simulations predict that the cosmic star formation rate density peaks at $z \geq 5$, unlike most of the semi-analytic models of galaxy formation (Nagamine et al. 2004b).
- (3) The above two facts suggest that there would be enough ionizing photons to reionize the Universe at $z = 6$ from the Pop II stars in ordinary galaxies.
- (4) The simulations overpredict the LAE LF by a factor of ~ 10 , and two different scenarios (‘uniform dimming’ and ‘random sampling’) can be considered to reconcile this result with the observed LF.
- (5) The ‘uniform dimming’ scenario has a stronger spatial correlation strength for LAEs than the ‘random sampling’ scenario, and this can be tested by direct comparison to the observed data.

In the ‘uniform dimming’ scenario, the LAE sample for a given Ly α luminosity cut would directly correspond to a sample of bright LBGs that are already observed by the 8 meter class telescopes and the Hubble Space Telescope. Therefore the ‘uniform dimming’ scenario suggests a strong link between the LAE and LBG sample, which can also be tested by comparing the spatial correlation function of the two samples at the same redshift. This observational test can be readily performed with the existing Subaru telescope data (Ouchi et al. 2004, 2005). In the real Universe, it is certainly possible that both effects of ‘uniform dimming’ and ‘random sampling’ may be at play. We also plan to perform direct comparisons of the simulated and the observed angular correlation functions of both LAEs and LBGs in a similar spirit to the work

by Hamana et al. (2004). The physical link between LAEs and LBGs can also be tested by a cross-correlation study of the two population.

References

- [1] Barton, E., Davé, R., *et al.* ApJ, 2004, **604**, L1
- [2] Bouwens, R., Illingworth, G. D., *et al.* ApJ, 2004, **606**, L25
- [3] Cen, R., Nagamine, K., Ostriker, J. P., 2005, ApJ, 635, 86
- [4] Cole, S., Lacey, C. G., *et al.* 2000, MNRAS, **319**, 168
- [5] Furlanetto, S. R., Schaye, J., *et al.* ApJ, 2005, **622**, 27
- [6] Hamana, T., Ouchi, M., *et al.* 2004, MNRAS, **347**, 813
- [7] Hernquist, L. & Springel, V., 2003, MNRAS, **341**, 1253
- [8] Kauffmann, G., Colberg, J. M., *et al.*, 1999, MNRAS, **303**, 188
- [9] Leitherer, K., Schaerer, D., *et al.*, 1999, ApJS, **123**, 3
- [10] Malhotra, S. & Rhoads, J. E., 2004, ApJ, **617**, L5
- [11] Menci, N., Cavaliere, A., *et al.*, 2002, ApJ, **575**, 18
- [12] Nagamine, K., Fukugita, M., *et al.* 2001, ApJ, **558**, 497
- [13] Nagamine, K., ApJ, 2002, **564**, 73
- [14] Nagamine, K., Springel, V., Hernquist, L., *et al.* 2004a, MNRAS, **350**, 385
- [15] Nagamine, K., *et al.* 2004b, ApJ, **610**, 45
- [16] Nagamine, K., *et al.* 2005a, ApJ, **618**, 23
- [17] Nagamine, K., *et al.* 2005b, ApJ, **627**, 608
- [18] Night, C., Nagamine, K., *et al.* 2006, MNRAS, 366, 705
- [19] Ouchi, M., Shimasaku, K., *et al.*, 2004, ApJ, **611**, 685
- [20] Ouchi, M., Shimasaku, K., *et al.*, 2005, ApJL, **620**, L1
- [21] Perlmutter, S., Aldering, G., *et al.*, 1999, ApJ, **517**, 565
- [22] Riess, A., Fillipenko, A. V., *et al.*, 1998, AJ, **116**, 1009
- [23] Ryu, D., Ostriker, J. P., Kang, H., & Cen, R., 1993, ApJ, **414**, 1
- [24] Somerville, R., Primack, J. R., Faber, S. M., 2001, MNRAS, **320**, 504
- [25] Spergel, D. N., Verde, L., *et al.*, 2003, ApJS, **148**, 175
- [26] Springel, V., 2005, MNRAS, 364, 1105
- [27] Springel, V. & Hernquist, L., 2002, MNRAS, **333**, 649
- [28] Springel, V. & Hernquist, L., 2003a, MNRAS, **339**, 289
- [29] Springel, V. & Hernquist, L., 2003b, MNRAS, **339**, 312